This is the peer reviewd version of the followng article:

Pull-in Instability Analysis of a Nanocantilever Based on the Two-Phase Nonlocal Theory of Elasticity / Mikhasev, G., Radi, E., Misnik, V.. - In: JOURNAL OF APPLIED AND COMPUTATIONAL MECHANICS. - ISSN 2383-4536. - 8:4(2022), pp. 1456-1466. [10.22055/JACM.2022.40638.3619]

Terms of use:

The terms and conditions for the reuse of this version of the manuscript are specified in the publishing policy. For all terms of use and more information see the publisher's website.

17/11/2026 17:26

(Article begins on next page)

J. Appl. Comput. Mech., xx(x) (2022) 1-11
DOI: 10.22055/jacm.2022.40638.3619

ISSN: 2383-4536
jacm.scu.ac.ir

Shahid Chamran University of Ahvaz

Journal of Applied and Computational Mechanics



Research Paper

Pull-in Instability Analysis of a Nanocantilever Based on the Two-Phase Nonlocal Theory of Elasticity

Gennadi Mikhasev[1], Enrico Radi[2], Vyacheslav Misnik[1]

[1] Department of Bio- and Nanomechanics, Belarusian State University, 4 Nezavisimosti Avenue, Minsk, 220140, Belarus, Email: mikhasev@bsu.by (G.M.)

[2] Dipartimento di Scienze e Metodi dell'Ingegneria, Università di Modena e Reggio Emilia, Via Amendola 2, Reggio Emilia, 42122, Italy, Email: eradi@unimore.it (E.R.)

Received April 24 2022; Revised May 31 2022; Accepted for publication June 11 2022.
Corresponding author: G. Mikhasev (mikhasev@bsu.by)
© 2022 Published by Shahid Chamran University of Ahvaz

Abstract. This paper deals with the pull-in instability of cantilever nano-switches subjected to electrostatic and intermolecular forces in the framework of the two-phase nonlocal theory of elasticity. The problem is governed by a nonlinear integro-differential equation accounting for the external forces and nonlocal effects. Assuming the Helmholtz kernel in the constitutive equation, we reduce the original integro-differential equation to a sixth-order differential one and derive a pair of additional boundary conditions. Aiming to obtain a closed-form solution of the boundary-value problem and to estimate the critical intermolecular forces and pull-in voltage, we approximate the resultant lateral force by a linear or quadratic function of the axial coordinate. The pull-in behavior of a freestanding nanocantilever as well as its instability under application of a critical voltage versus the local model fraction are examined within two models of the load distribution. It is shown that the critical voltages calculated in the framework of the two-phase nonlocal theory of elasticity are in very good agreement with the available data of atomistic simulation.

Keywords: Nano-switch, nanocantilever, two-phase nonlocal theory, intermolecular forces, pull-in instability.

1. Introduction

Micro- or nanocantilevers are often used as sensing elements in various kinds of MEMS and NEMS and, in particular, in capacitive sensors and switches [1-7]. Consider a typical beam-type electrostatic nanoscale switch. It consists of a nanocantilever beam electrode suspended above a stationary conductive ground electrode [7]. Under an applied voltage, the flexible beam electrode deflects towards the fixed one, and when the voltage reaches a critical value, called as pull- in voltage, the movable electrode collapses onto the substrate. This phenomenon, known as pull-in instability, is the subject of numerous studies aimed at determining the critical voltage, which is very sensitive to all physical and geometric parameters characterizing the nanoscale device. Indeed, if the gap between the electrodes is too small, a cantilever beam may deflect and stick to the fixed electrode due to the intermolecular forces even if no voltage is applied [8]. The effects of van der Waals (vdW) and Casimir forces on the pull-in instability of nanocantilevers were studied by many researchers (among many others, see [9-18]). These forces originate from the electrostatic interaction among dipoles and act between bodies separated by a few micrometres (μm) to nanometers (nm). Both forces refer to the same physical phenomenon and thus they do not act simultaneously. The main difference between them consists in their range of applicability. Indeed, van der Waals forces act at separation distances shorter than few tens of nanometers, while the Casimir forces prevail at larger distances, and the transition from these forces occurs smoothly. With reference to the simple geometry of two parallel plates the magnitude of the van der Waals forces is inversely proportional to the third power of the separation distance, whereas that of the Casimir forces is inversely proportional to the fourth power. Therefore, the analytical expression of the intermolecular forces may change as the nanocantilever deflection increases. With the increasing miniaturization of devices, the effects of the intermolecular forces become more and more important. In particular, they may cause a significant reduction of the pull-in voltage as the size of the device decreases. These forces are also responsible for the stiction phenomenon that may occur in a nanocantilever switch when their magnitudes overcome the restoring elastic forces, thus keeping the flexible electrode attached to the ground, also in the absence of electrostatic actuation. The occurrence of stiction is exploited in applications such as nonvolatile memory cells, where the switch is held in the closed state with no need for continued power input. However, in applications such as nanoresonators and nanoactuators it may lead to permanent adhesion and other undesirable consequences, which may limit the functionality of the device.

Very small dimensions of 1D and 2D bodies exploited as sensing elements of MEMS/NEMS make it necessary to take into account both the small scale effects and intermolecular forces acting between components of a nanostructure. To date, there are many papers studying the phenomena caused by small sizes (among many others, see [19-23]). In particular, examining nonlinear oscillations of a CNT nanoresonator, Goharimanesh and Koochi [19] showed that the Casimir forces reduce the nanoresonator frequencies, while the nonlocal parameter has a hardening effect and enhances the system's frequency. Malikan et al. [20] analyzed

Published online: June 21 2022

buckling of a non-concentrated double-walled carbon nanotube taking the van der Waals interaction between inner and outer tubes into account, within the nonlocal strain gradient theory of elasticity. Applying the nonlocal elasticity theory, Dastjerdi and Malikan [21] simulated nonlinear bending analysis of an eccentric defected bilayer graphene sheets considering the effect of van der Waals forces, and Sedighi et al. [22] and Jena et al. [23] adopted this theory to study vibrations of hybrid composite nanotubes and functionally graded porous nanobeam embedded in an elastic foundation. Koochi et al. [24] examined the dynamic instability of a CNT nano-sensor taking into account the impacts of the material length scale, van der Waals forces, damping and the longitudinal magnetic field. Moreover, the mechanical behavior of nanosize beams is studied within nonlocal elasticity also in some other related papers [25-27], where different physical effects are considered, like a varying heat source and a dynamic load [25], and magneto-elastic phenomena [26, 27].

As for the problem of pull-in instability of nano-switches, to date there are only a few papers taking into account both nonlocal phenomenon and intermolecular forces induced by small sizes [28-33]. The modified couple stress theory was introduced in [28, 29] to demonstrate the effects of dispersion forces and size dependence on the pull-in instability of cantilever micro- and nanobeams. Based on the so-called modified strain gradient theory, Taati and Sina [30] considered the static pull-in behavior of electrostatically actuated functionally graded micro-beams resting on an elastic foundation, whose nonlinear governing equation was solved using an iterative numerical method being a combination of the fourth-order Runge–Kutta and shooting methods. The Eringen nonlocal theory [34, 35] was used in papers [31-33] to consider the effect of the internal length scale. In particular, introducing the nonlocality scale parameter and assuming a linear distribution of the resultant external force acting on a cantilever, Yang et al. [31] obtained a closed-form solution. Mousavi et al. [32] solved the same problem numerically by differential quadrature method, and Sedighi and Sheikhanzadeh [33] used this method for investigating the static and dynamic pull-in behavior of nanobeams resting on the elastic foundation. An interesting experimental study was carried out by Sadeghian et al. in [36], where the phenomenon of electrostatic pull-in instability was used to estimate the size-dependent effective Young's modulus of silicon nanocantilevers.

The main conclusion of most of the aforementioned studies is that an increase in the small scale factor leads to higher pull-in voltage and allows eliminating the gap between the experimental observations and data predicted by various theoretical approaches. It should be noted that when claiming the use of Eringen's theory [34, 35], which originally has an integral form, most authors actually set the problem within the framework of the stress gradient model of the nonlocal elasticity theory. However, such a differential approach does not allow capturing the nonlocal effects in a neighborhood of the beam edges [37], especially when boundary conditions are set in the terms of stresses [38, 39].

Motivated by the mentioned drawback of available studies on the pull-in behavior of a nanocantilever within the Eringen's theory, we aim to perform the pull-in instability analyses of a nanocantilever based on the two-phase nonlocal (TPNL) model of elasticity [34, 35]. This model combines the purely nonlocal (PNL) model of elasticity with classical elasticity and is immune from the inconsistencies of the PNL model [40].

The paper is organized as follows. First, following TPNL theory of elasticity [34, 35], we set the problem in Section 2 in integro-differential form introducing the local and nonlocal volume fractions in the constitutive equations. In Section 3, assuming the Helmholtz kernel in the constitutive equation, we reduce the nonlinear integro-differential equation accounting both for electrostatic and intermolecular forces to the so-called "equivalent" differential equation of the sixth order and we derive a pair of additional boundary conditions accounting for nonlocal effects near the edges. Two approximated models of the distributed lateral force acting on the beam, obtained by assuming linear or quadratic load distributions, are proposed in Section 4. Calculations of critical intermolecular forces and applied voltage resulting in the pull-in instability of a nanobeam versus the local model fraction for the linear and quadratic distributions of the external force are given in Sections 5 and 6. The comparative analysis of our results with outcomes of atomistic simulations by Dequesnes et al. [41] is also presented in Section 6. Finally, in Section 7, we draw some conclusions regarding the scale effect on the pull-in behavior of electrostatic nanoscale switches.

2. Mathematical Model

Consider a micro/nano-switch consisting of a fixed electrode and a micro/nanocantilever of length L, width b and thickness h separated by a dielectric spacer with an initial gap g, as shown in Fig. 1. A voltage V applied to the electrode yields a distributed electrostatic load F_e acting on the cantilever. This force together with an intermolecular force F_m, where $m = 3$ and $m = 4$ correspond to the van der Waals and the Casimir forces, respectively, result in the deflection $w(x)$ of the beam towards to the electrode. At a critical voltage value, called the pull-in voltage, the phenomenon of the pull-in instability of the nano-switch occurs, which consists in the retraction of the cantilever onto the stationary electrode.

For the flexural beam, the vertical equilibrium implies the following equation

$$\frac{d^2M}{dx^2} = -q(x), \tag{1}$$

where M is the bending moments, and $q(x) = F_e + F_m$ is the distributed lateral load per unit length. The electrostatic force, including the fringing one, and the van der Waals (vdW) and Casimir forces as well are given by:

$$F_e = \frac{\varepsilon_0 b V^2}{2(g-w)^2}\left(1 + 0.65\frac{g-w}{b}\right), \quad F_3 = \frac{Ab}{6\pi(g-w)^3}, \quad F_4 = \frac{\pi^2 \bar{h} c b}{240(g-w)^4} \tag{2}$$

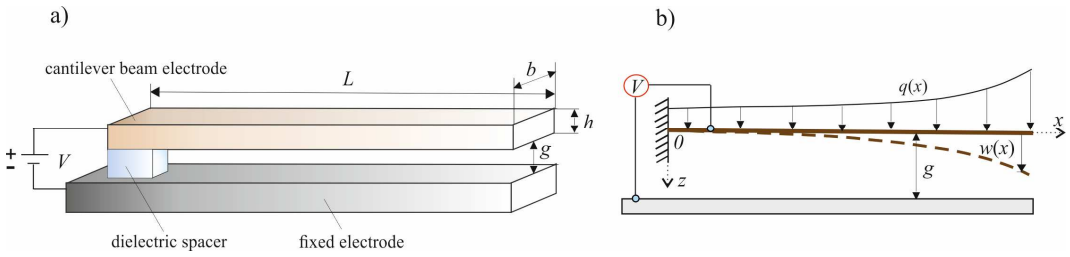


Fig. 1. Schematic configuration of a nano-switch (a). Cantilever beam model of a nano-switch (b).

where $\varepsilon_0 = 8.854 \cdot 10^{-12} \mathrm{C^2 N^{-1} m^{-2}}$ is the permittivity of vacuum, A is the Hamaker constant, $\overline{h} = 1.055 \cdot 10^{-34}\,\mathrm{Js}$ is the Plank's constant divided by 2π, and $c = 2.998 \cdot 10^8\,\mathrm{m/s}$ is the speed of light. The boundary conditions for the cantilever read

$$w(0) = w'(0) = 0, \quad M(L) = M'(L) = 0\,, \tag{3}$$

where prime means the derivative with respect to the x-coordinate.

In the framework of the local theory of elasticity, the bending moment is defined as $M = -EI\,w''$, where EI is the bending rigidity of the beam. In accordance with the TPNL model of elasticity, we have [37, 38]

$$M = -EI\left(\xi_1 \frac{d^2 w}{dx^2} + \xi_2 \int_0^L K\left(|x-\hat{x}|,\kappa\right) \frac{d^2 w}{d\hat{x}^2}\, d\hat{x}\right), \tag{4}$$

where $K(|x-\hat{x}|,\kappa)$ is the attenuation kernel, κ is the internal length scale parameter, and ξ_1, ξ_2 are the volume fractions corresponding to the local and nonlocal phases, such that $\xi_1 + \xi_2 = 1$ and $\xi_1 \xi_2 > 0$. The kernel K is the positive, symmetric function, which rapidly decays far from x and satisfies the condition

$$\int_R K\left(|x-\hat{x}|,\kappa\right) d\hat{x} = 1\,. \tag{5}$$

Equation (1) with the constitutive relation (4) then provide an integro-differential governing equation. The boundary conditions (3) for the free edge $x = L$ also take the integro-differential form. If $\xi_2 = 0$, then the problem degenerates into the classical local form considered earlier in many papers [9-15].

3. Reduction of the Problem to the Differential Form

In our study we assume the Helmholtz kernel

$$K\left(|x-\hat{x}|,\kappa\right) = \frac{1}{2\kappa} \exp\left(-\frac{|x-\hat{x}|}{\kappa}\right), \tag{6}$$

which is frequently used for 1D nanosized objects and allows for reducing the above stated problem to the purely differential form.

First, we introduce the dimensionless quantities

$$\begin{aligned} &s = \frac{x}{L}, \quad u = \frac{w}{g}, \quad \mu = \frac{\kappa}{L}, \quad \beta = \frac{\varepsilon_0 b V^2 L^4}{2g^3 EI}, \\ &\gamma = 0.65\frac{g}{b}, \quad \alpha_3 = \frac{AbL^4}{6\pi g^4 EI}, \quad \alpha_4 = \frac{\pi^2 \overline{h} c b L^4}{240 g^5 EI}. \end{aligned} \tag{7}$$

The substitution of (2) into Eq. (1), taking Eqns. (4)-(7) into account, results in the integro-differential equation in dimensionless form

$$\xi_1 \frac{d^4 u}{ds^4} + \frac{\xi_2}{2\mu} \frac{d^2}{ds^2} \int_0^1 e^{-\frac{|s-\hat{s}|}{\mu}} \frac{d^2 u}{d\hat{s}^2}\, d\hat{s} = f(u) \tag{8}$$

with

$$f(u) = \frac{\gamma\beta}{1-u} + \frac{\beta}{(1-u)^2} + \frac{\alpha_3}{(1-u)^3} + \frac{\alpha_4}{(1-u)^4}\,. \tag{9}$$

We will seek a solution of Eq. (8) on the set of functions $u \in C^6[0,1]$. Performing the mathematical manipulations with Eq. (8) as done in [38], we get the following sixth-order differential equation:

$$\mu^2 \xi \frac{d^6 u}{ds^6} - \frac{d^4 u}{ds^4} = \mu^2 \frac{d^2 f(u)}{ds^2} - f(u), \tag{10}$$

where $\xi = \xi_1$.

The main boundary conditions (3) can be also rewritten in the purely differential form [38], the first pair of conditions at the left end remaining the same as in the classical problem

$$u(0) = u'(0) = 0, \tag{11}$$

while the second pair for the right edge becomes:

$$\begin{aligned} M(L) = 0 \quad &\Rightarrow \quad \mu^2 \xi\, u^{IV}(1) - u''(1) - \mu^2 f(u_T) = 0, \\ M'(L) = 0 \quad &\Rightarrow \quad \mu^2 \xi\, u^{IV}(1) + \mu\xi\, u'''(1) - (1-\xi) u''(1) - \mu^2 f(u_T) = 0, \end{aligned} \tag{12}$$

where $u_T = u(1)$ is the dimensionless tip deflection of the nanocantilever.

Owing to double differentiation of the original integro-differential Eq. (8), the derived purely differential Eq. (10) might have spurious solutions. To rule them out, one needs to impose additional boundary conditions (the so-called constitutive conditions [42]). Indeed, by differentiating the original Eq. (8) once with respect to s and then evaluating it at the beam edges, one arrives at the following pair of conditions:

$$\begin{aligned} &\mu^3 \xi\, u^{V}(0) - \mu^2 \xi\, u^{IV}(0) - (1-\xi)\left[\mu\, u'''(0) - u''(0)\right] = -\mu^2 f(0) + \mu^3 f_s'(0), \\ &\mu^3 \xi\, u^{V}(1) + \mu^2 \xi\, u^{IV}(1) - (1-\xi)\left[\mu\, u'''(1) + u''(1)\right] = \mu^2 f(u_T) + \mu^3 f_s'(u_T), \end{aligned} \tag{13}$$

with $f_s' = df/ds$.

Therefore, the cantilever deflection u follows from the solution of the boundary-value problem (10)-(13). Then, to calculate the pull-in voltage, it becomes necessary to find the maximum positive value of the parameter β for which $u_T < 1$. For $\mu = 0$ and $\xi = 1$ this problem degenerates into the problem of a macro-sized cantilever, which was studied in many papers (among many others, see in [9, 14, 15]). Assuming $\xi = 0$ and omitting the additional boundary conditions (13), we obtain the problem (10)-(12) considered by Yang et al. [31] within Eringen's stress gradient theory. However, we note that the problem considered in [31] is not equivalent to the problem formulated above as $\xi \to 0$. Indeed, the boundary-value problem (10)-(13) is singularly perturbed because it contains a small parameter ξ by the highest derivatives, both in the governing equations and boundary conditions. As $\xi \to 0$, the singular problem (10)-(13) degenerates into a problem with boundary conditions not coinciding with the original boundary conditions being formulated within the PNL model of elasticity. We do not discuss here the link between these two problems formulated within TPNL and PNL models (e.g., see some discussions related to nanorods in [43]) as well as ill-posedness of PNL models and refer to paper [40].

4. Simplified Models Based on the Approximation of the Lateral Force

Due to the nonlinearity of the external force experienced by the cantilever, problem (10)-(13) does not allow an exact solution in the explicit form. We use here an approach based on the approximation of the lateral force by a linear or quadratic function of the nondimensional abscissa s, namely

$$f(s) = f[u(s)] = f_0 + (f_T + f_0)s^n, \tag{14}$$

where $n = 1, 2$ and $f_0 = \beta + \gamma\beta + \alpha_3 + \alpha_4$. We note that the case $n = 1$ at $f(0) = f_0 = 0$ was earlier considered by Yang et al. [31] when studying a nanobeam in the framework of the stress gradient theory of nonlocal elasticity.

4.1 Linear Distributed Load Model

Consider the linear distributed load (LDL) model with $n = 1$ in (14). Substituting (14) into Eq. (10) and integrating four times, we arrive at the following equation

$$\mu^2\xi u'' - u = \sum_{k=0}^{4}\frac{1}{k!}a_k s^k - \frac{1}{24}f_0 s^4 - \frac{f_T - f_0}{120}s^5, \tag{15}$$

where α_k are arbitrary constants. Its general solution reads

$$u = \sum_{k=0}^{5} c_k s^k + a_4 e^{\frac{s}{\mu\sqrt{\xi}}} + a_5 e^{-\frac{s}{\mu\sqrt{\xi}}} \tag{16}$$

with

$$\begin{aligned} &c_0 = \mu^2\xi\left(\mu^2\xi f_0 - a_2\right) - a_0, \quad c_1 = \mu^2\xi\left[\mu^2\xi(f_T - f_0) - a_3\right] - a_1, \quad c_2 = \frac{1}{2}\left(\mu^2\xi f_0 - a_2\right), \\ &c_3 = \frac{1}{6}\left[\mu^2\xi(f_T - f_0) - a_3\right], \quad c_4 = \frac{1}{24}f_0, \quad c_5 = \frac{1}{120}(f_T - f_0). \end{aligned} \tag{17}$$

Note that, if the nanocantilever deflection under the actual distributed load is expected to be a convex function, then the approximation of the distributed load with a linear function having the correct values at $s = 0$ and $s = 1$ turns out to overestimate the actual load distribution. To decrease the total load acting on the nanocantilever with respect to the linear distribution, then a quadratic load distribution is also considered in the following.

4.2 Quadratic Distributed Load Model

For $n = 2$, namely for the quadratic distributed load (QDL) model, Eq. (10) has the following general solution

$$u = \sum_{k=0}^{6} c_k s^k + a_4 e^{\frac{s}{\mu\sqrt{\xi}}} + a_5 e^{-\frac{s}{\mu\sqrt{\xi}}}, \tag{18}$$

where

$$\begin{aligned} &c_0 = \mu^4\xi(\xi - 1)(f_T - f_0) - \mu^2\xi a_2 - a_0, \quad c_1 = -\mu^2\xi a_3 - a_1, \quad c_2 = \mu^2(\xi - 1)(f_T - f_0) - \frac{1}{2}a_2, \\ &c_3 = -\frac{1}{6}a_3, \quad c_4 = \frac{\mu^2}{12}(\xi - 1)(f_T - f_0), \quad c_5 = 0, \quad c_6 = \frac{1}{360}(f_T - f_0). \end{aligned} \tag{19}$$

4.3 Equation for Estimation of Pull-in Voltage

Regardless of the model assumed, let the function $u(s; a_0, a_1, \ldots, a_5; f_T)$ denote the general solution of problem (10)-(13), which depends on six constants α_k $(k = 1, \ldots, 6)$ and the unknown parameter f_T corresponding to the force at the cantilever tip. The six constants α_k are readily found from the boundary conditions (11)-(13). Let us denote with $u^*(s; f_T)$ the solution of problem (10)-(13), evaluated by relations (16), (17) or (18), (19). Then, the tip deflection u_T will be a function of f_T:

$$u_T = u^*(1; f_T). \tag{20}$$

As it follows from (9), the force at the cantilever tip is

$$f_T = \frac{\beta}{1 - u_T} + \frac{\gamma\beta}{(1 - u_T)^2} + \frac{\alpha_3}{(1 - u_T)^3} + \frac{\alpha_4}{(1 - u_T)^4}. \tag{21}$$

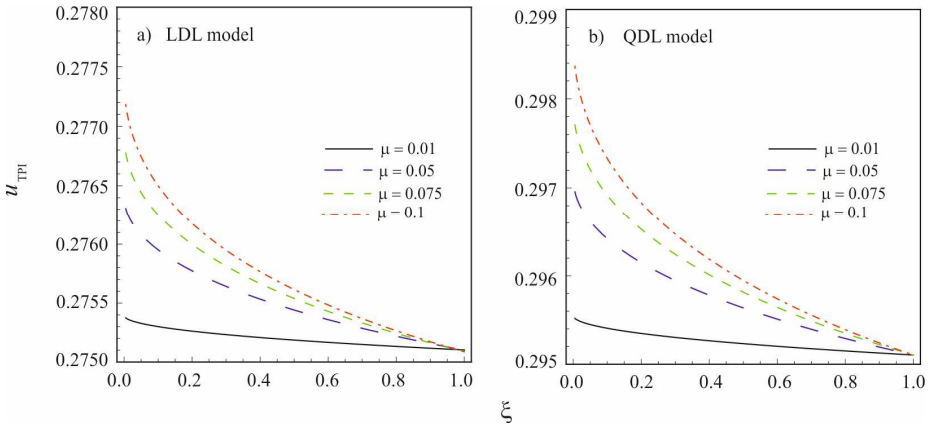


Fig. 2. Tip deflection u_{TPI} of a freestanding cantilever nanobeam versus the local model fraction ξ based on LDL (a) and QDL (b) models taking the van der Waals force (m = 3) into account, for different values of the dimensionless internal length scale parameter μ.

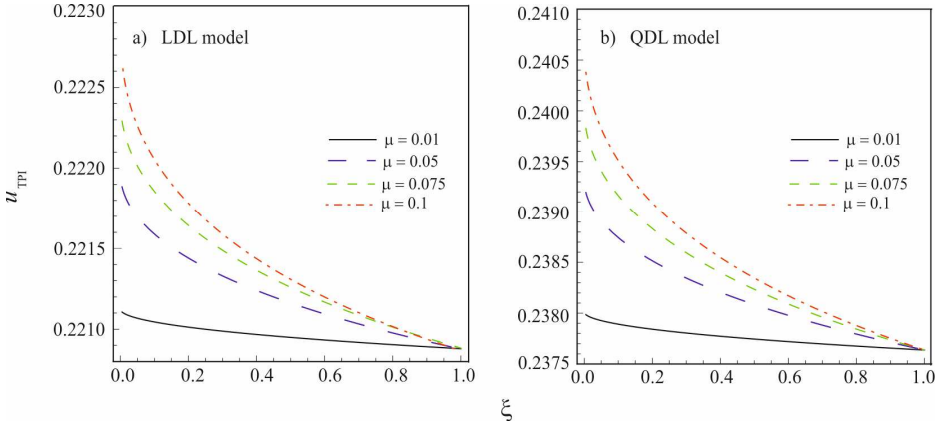


Fig. 3. Tip deflection u_{TPI} of a freestanding cantilever nanobeam versus the local model fraction ξ evaluated on the base of LDL (a) and QDL (b) models taking the Casimir force (m = 4) into account, for different values of the dimensionless internal length scale parameter μ.

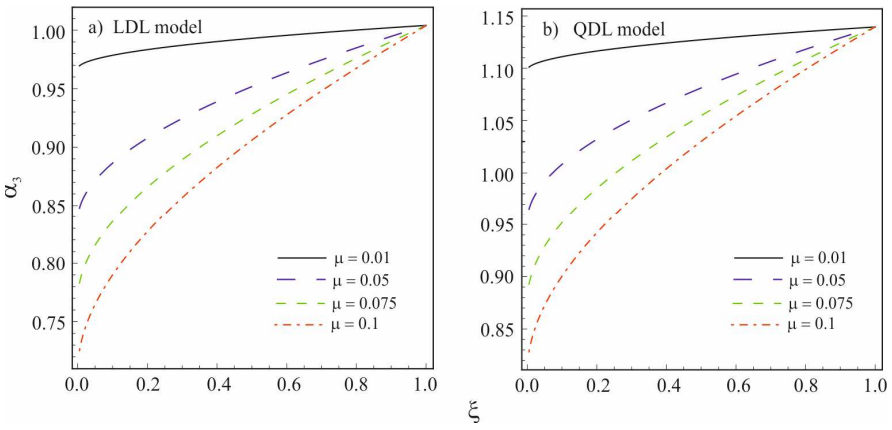


Fig. 4. Dimensionless parameter α_3 for a freestanding cantilever nanobeam versus the local model fraction ξ evaluated on the base of LDL (a) and QDL (b) models taking the van der Waals force (m = 3) into account, for different values of the dimensionless internal length scale parameter μ.

The substitution of (21) into the right-hand side of Eq. (20) yields the relationship $\beta = \beta(u_T)$. The extreme value β_{PI} corresponding to the pull-in instability and associated maximum amplitude of the cantilever tip can be found from the condition $d\beta/du_T = 0$.

5. Freestanding Nanocantilever

When the gap between the fixed electrode and the nanobeam is very small and the cantilever is long enough, it may fall onto the base due to the intermolecular forces. For correctly designing a nano-switch in NEMS devices, it becomes very important to estimate the optimal geometrical parameters and to predict a deflection of a nanobeam accounting for the intermolecular forces. Relying on the condition $d\alpha_m/du_T = 0$, we calculated the critical value α_{mPI} of a parameter α_m (m = 3, 4) and the associated tip

displacement, u_{TPI}, versus the local model fraction ξ based on LDL (n = 1) and QDL (n = 2) models for different values of the dimensionless internal length scale parameter μ = 0.01, 0.05, 0.075, 0.1. The tip deflections u_{TPI} caused by van der Waals forces based on two different models are presented in Fig. 2. The analogous plots of u_{TPI} generated by Casimir forces are shown in Fig. 3. The associated critical values $\alpha_{3PI}, \alpha_{4PI}$ of parameters α_3 and α_4 are given in Figs. 4 and 5, respectively. In all cases, the calculations were performed for $\beta = 0, \gamma = 1$.

Figures 2 - 5 show that decreasing the internal length scale parameter μ and/or increasing the local model fraction ξ (that corresponds to the transition to the macro-scale model) results in decreasing the tip deflection u_{TPI} caused by the intermolecular forces and in increasing the parameters α_3 and α_4. It is seen that QDL model gives higher values both of the tip deflection and parameters α_m than the LDL model. This outcome allows considering the LDL model as the one predicting the upper bound for the tip deflection corresponding to the pull-in instability, since a linear distribution of the loading definitely overestimates the actual distribution. The curves plotted in Fig. 4 and 5 make it possible to estimate the freestanding nanobeam length and the gap between it and the fixed electrode. From Eqs. (7) it follows:

$$\frac{L}{g} < \sqrt[4]{\frac{\pi \alpha_{3PI} E h^3}{2A}} \quad \text{(for the nanobeam subjected to the van der Waals force),} \tag{22}$$

$$L < \sqrt[4]{\frac{20\alpha_{4PI} E h^3 g^5}{\pi^2 \bar{h}\, c}}, \quad g > \sqrt[5]{\frac{\pi^2 \bar{h} c L^4}{20\alpha_{4PI} E h^3}} \quad \text{(for the nanobeam subjected to the Casimir force).} \tag{23}$$

The parameters α_{3PI} and α_{4PI} are taken from Fig. 4 or Fig. 5, depending on the model assumed, for the fixed values of ξ and μ.

6. Pull-in Voltage

In this section we give the results of calculations of the critical parameter β_{PI} and the corresponding displacement u_{TPI} of the cantilever tip relying on LDL and QDL models taking the intermolecular forces into account. Computations were made for $\gamma = 1, \mu = 0.05$ at different values of the parameters ξ and α_m, where m =3, 4 correspond to the van der Waals and Casimir forces, respectively. Figs. 6 and 7 are obtained for m = 3 and Figs. 8 and 9 refer to m = 4. It is clearly seen that the QDL model gives higher values for the pull-in voltage with respect to LDL model, since in the latter model the loading distribution is overestimated and thus the pull-in voltage provided by the LDL model may be assumed as a lower bound to the effective pull-in voltage. Regardless both the model assumed and the type of an intermolecular force, the critical value β_{PI} corresponding to the pull-in voltage is an increasing functions of ξ, but a decreasing one of the parameter α_m. As the parameter β_{PI} is known, the required pull-in voltage V_{PI} is defined as

$$V_{PI} = \sqrt{\frac{E(gh)^3 \beta_{PI}}{6\varepsilon_0 L^4}} \tag{24}$$

When comparing the effects of different intermolecular forces on the pull-in voltage, one can conclude that at the same geometrical parameters and the local model fraction ξ, the pull-in voltage of a nanobeam under the Casimir force is much lower than under the van der Waals force that is in full agreement with outcomes of previous studies (e.g., see in [31]). An unexpected result is the behavior of the tip deflection u_{TPI} as a function of the local model fraction ξ under applied voltage and different intensity of the intermolecular force: there is a special value $\alpha_m = \alpha^*_m$ for which the tip deflection is weakly independent of ξ, for $\alpha_m < \alpha^*_m$ the deflection u_{TPI} decreases as ξ increases, and for $\alpha_m > \alpha^*_m$ the tip deflection increases together with the local model fraction ξ. Because the parameter α_m is strongly affected by the nanobeam length and initial gap, one can conclude that there exist some geometrical parameters, L^*, g^*, for which the profile of the nanobeam subjected to the critical electrostatic force is weakly influenced by the parameter ξ.

Figure 10 displays the effects of varying gap ratio g/b and the local model fraction ξ on the pull-in voltage evaluated on the basis of LDL model with the Casimir force taken into account. The data used in this numerical example are L = 200 nm, b = 30 nm, h = 3,5 nm, E = 166 GPa, $\mu = 0.1, \alpha = 0$. The values of the pull-in voltage V_{PI} calculated by Yang et al. [31] for the same parameters but relying on the Eringen's stress gradient model are also depicted in Fig. 10. It is seen that the results based on these two different approaches are in very good correlation for some value of the parameter ξ. In particular, for $\mu = 0.1$, our outcomes and those obtained by Yang et al. [31] turn out to be close for the local model fraction ξ varying from 0.5 to 0.75. However, for ξ < 0.25 the stress gradient model [31] gives overestimated values of V_{PI} with respect to the values found here within TPNL theory.

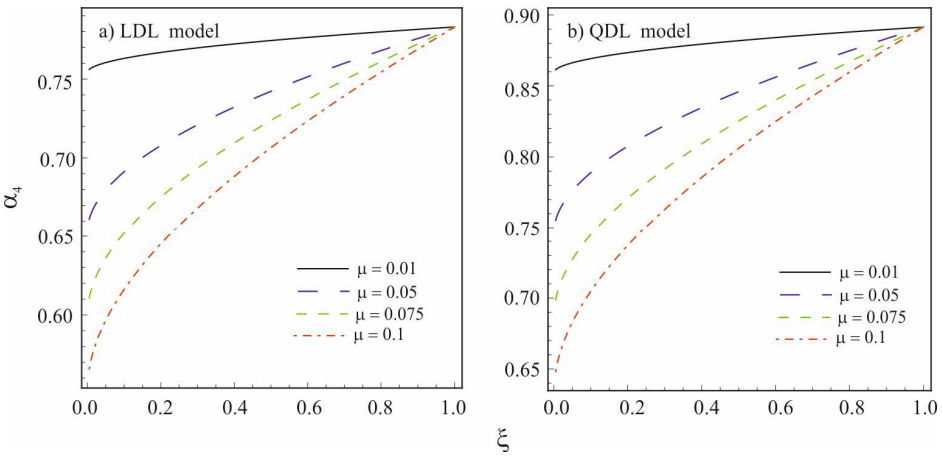


Fig. 5. Dimensionless parameter α_4 for a freestanding cantilever nanobeam versus the local model fraction ξ evaluated on the base of LDL (a) and QDL (b) models taking the Casimir force (m = 4) into account, for different values of the dimensionless internal length scale parameter μ.

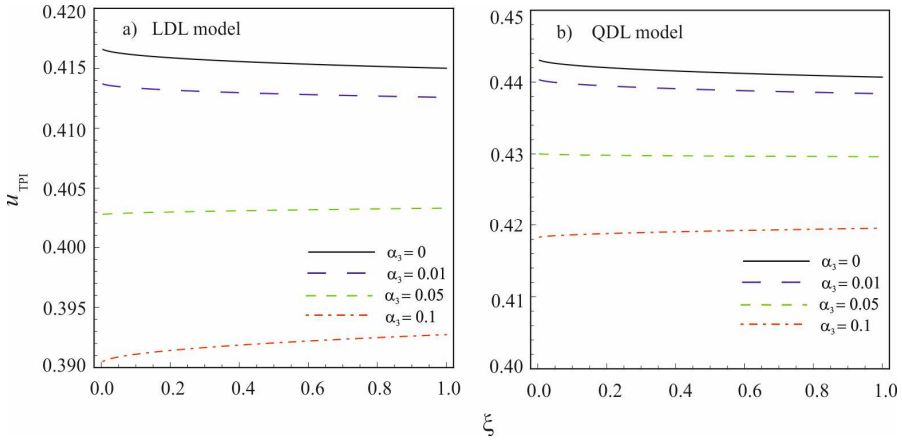


Fig. 6. Tip deflection u_{TPI} of a cantilever nanobeam versus the local model fraction ξ evaluated on the base of LDL (a) and QDL (b) models taking the van der Waals force (m = 3) into account, for different values of the parameter α_3.

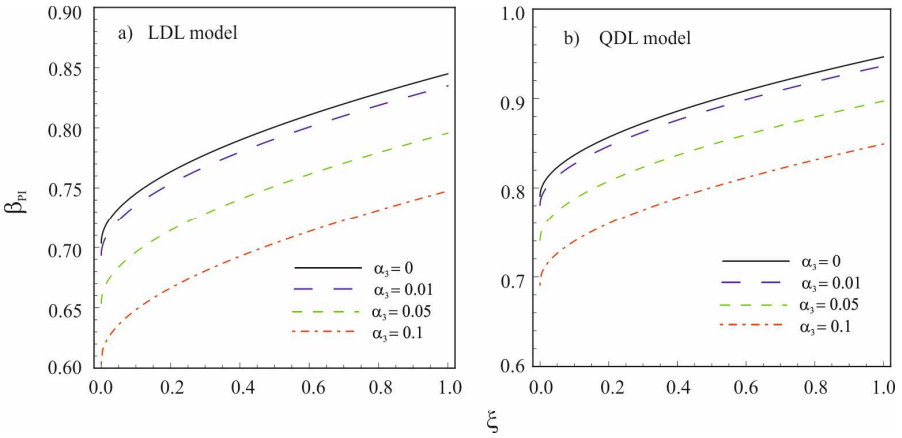


Fig. 7. Dimensionless parameter β_{PI} of the pull-in voltage for a cantilever nanobeam versus the local model fraction ξ evaluated on the base of LDL (a) and QDL (b) models taking the van der Waals force (m = 3) into account, for different values of the parameter α_3.

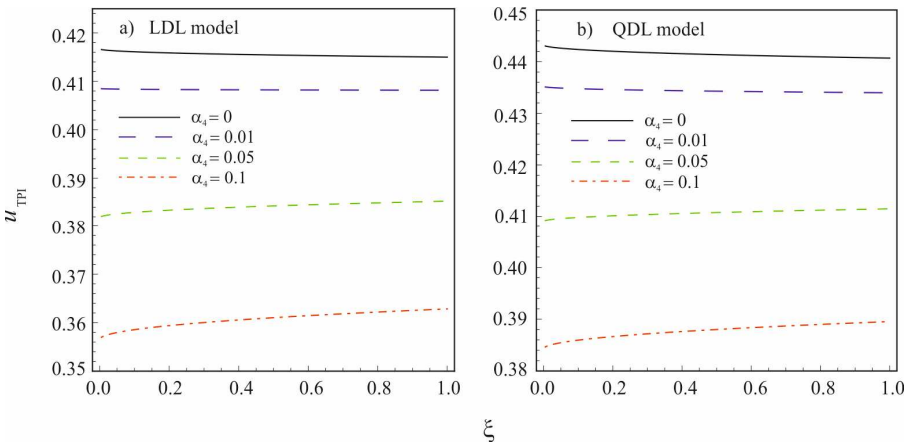


Fig. 8. Tip deflection u_{TPI} of a cantilever nanobeam versus the local model fraction ξ evaluated on the base of LDL (a) and QDL (b) models taking the Casimir force (m = 4) into account, for different values of the parameter α_4.

The accuracy of our models can be also verified by comparing their predictions with available data of atomistic simulations (AS). Following Dequesnes et al. [41], we consider a double-wall carbon nanotubes (DWCNT) suspended over a graphitic electrode and an equivalent nanocantilever with a rectangular cross-section. The width b and the thickens h of the nanobeam cross section are chosen so that its moment of inertia is equal to that of the DWCNT [41]:

$$I = \frac{\pi}{4}\left(R_{ext}^4 - R_{int}^4\right), \tag{25}$$

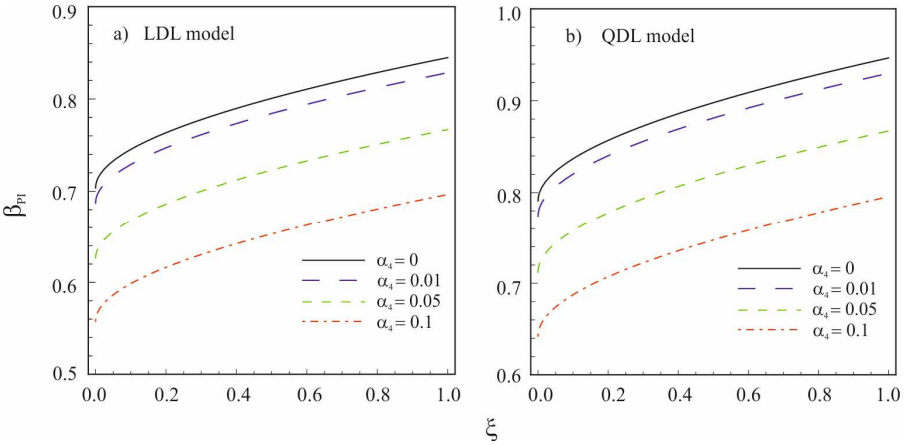


Fig. 9. Dimensionless parameter β_{PI} of the pull-in voltage for a cantilever nanobeam versus the local model fraction ξ evaluated on the base of LDL (a) and QDL (b) models taking the Casimir force ($m = 4$) into account, for different values of the parameter α_4.

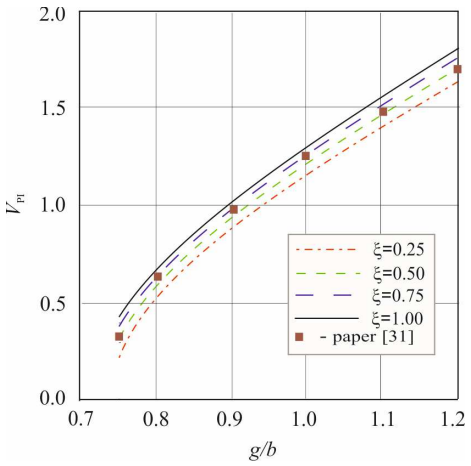


Fig. 10. Pull-in voltage V_{PI}, evaluated accounting for the Casimir force on the basis of LDL model, versus the gap ratio g/b for a cantilever nanobeam with different values of the local model fraction ξ.
Pull-in voltages found within the Eringen's stress gradient model [31] are marked in the plot.

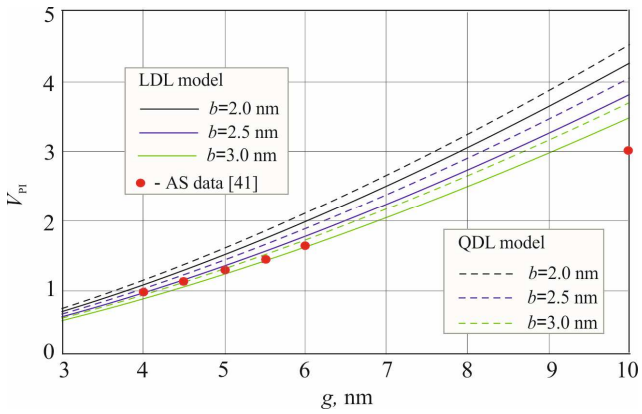


Fig. 11. Pull-in voltage V_{PI}, evaluated based on the LDL and QDL models neglecting the intermolecular forces, versus the gap g for cantilever nanobeams of various widths b. Pull-in voltages found by the atomistic simulation [41] are marked in the plot.

where R_{ext} and R_{int} are the exterior and interior radii of the DWCT, respectively. It is worth noting that AS performed in [41] closely matched results of both numerical calculations based on the equivalent continuum model and the experimental data reported for carbon-nanotube-based nano-switches and nano-tweezers [44]. The Young's modulus of CNT is taken to be $E = 1.2$ TPa, which is consistent with the theoretical and experimental data [45-47]. The DWCNT is 50 nm long and has the radii $R_{ext} = 1$ nm, $R_{int} = 0.665$ nm, which are the same as in [41]. The internal length scale parameter is calculated as $\kappa = e_0 a$, where e_0 is the material constant of nonlocality and $a = 0.142$ nm is the length of the C-C bond for a single walled carbon nanotube [49]. Here, we assume $e_0 = 0.39$, as given by Eringen [48], then the small parameter $\mu = 0.001$ follows from (7)3. In Figure 11, the analytical pull-in voltage calculated both for the LDL and QLD models neglecting the contribution of intermolecular forces is shown as a function of the initial gap g for different width of the equivalent beam. The curves displayed in Fig. 11 were plotted for the local model fraction $\xi = 0.1$. We note that for $\mu = 0.001$ outcomes of calculations performed within TPNL theory are weakly dependent on the parameter

ξ. The data of the AS performed in [41] are also plotted in Fig. 11 for six available values of the initial gap. The uneven distribution of the AS points in Fig. 11 (as well as in Fig. 12) is explained by the fact that the corresponding points in Fig. 12 obtained from paper [41] were depicted in a coordinate system with a logarithmic scale. It may be observed that the theoretical values of the pull-in voltage calculated on the basis of TPNL theory and within the framework LDL/QDL models depend on the chosen nanobeam width: for very narrow nanobeam both models give similar results, which are close to the AS data.

However, the theoretical outcomes begin to diverge and turn to be higher the AS point as the initial gap g increases. For b = 3 nm, the best matching between the theoretical results and the AS data is provided by the QLD model for the initial gap g varying in the range between 3 and 5 nm, and for b > 5 nm, the LDL model gives the best results.

The vdW or Casimir forces are taken into account in the plots depicted in Fig. 12. Calculations were carried out only for b = 3 nm both for the LDL and QDL models. Since the Casimir forces prevail at larger distances, we plotted the corresponding curves for a relatively large value of the initial gap. The dotted red line is the result of interpolation based on the available AS data. One can see that there is a critical value of the initial gap $b = b^*$ provided by the LDL or QDL models, such that for $b \le b^*$ the cantilever is unstable in the absence of electrostatic actuation. The analysis of plots presented in Fig. 12 allows drawing the following conclusions. For the chosen value of the beam width b ensuring the same moment of inertia of the beam cross-section as for the carbon nanotube, the best matching between our results and the AS data strongly depends on the assumed model (LDL or QDL) and the initial gap g. For very small value of the initial gap, the best matching to the AS outcomes is assured by the LDL model accounting for vdW forces, while for large values of g this model results in errors with respect to the AS data. In its place, the QLD model might be used for estimating the pull-in voltage by taking the Casimir forces into account, for values of the initial gap lying in the range from 9 to 11 nm. Since the atomistic simulation in [41] was carried out only for $g \le 10$ nm, the accuracy of the QDL model within the TPNL theory of elasticity for larger values of the initial gap has to be the subject of further investigations.

7. Conclusion

The effects of nonlocal material behavior on the pull-in instability of a nanocantilever switch was investigated here by using the TPNL model of elasticity and taking the intermolecular forces into account. The original integro-differential problem was reduced to a differential governing equation of the sixth order. The additional boundary conditions were properly derived, thus making the model free from the inconsistencies of the PNL model. The problem was strongly nonlinear since the loading distribution depends on the beam deflection. To make the problem analytically tractable, two levels of approximation were introduced on the distributions of the electrostatic and intermolecular forces along the nanobeam axial coordinate, which were assumed in the form of a linear or quadratic function. While the linear distribution generally overestimated the actual loading distribution and thus provided a lower bound to the pull-in voltage, the quadratic loading distribution could provide better approximated results for some ranges of the material and geometric parameters, in particular for large initial gaps. The effect of nonlocal material behavior mainly consisted in an increase in the pull-in voltage and in the freestanding length of the nanocantilever as a consequence of the increase in the critical level of the intermolecular forces causing the collapse of the switch in the absence of electrostatic actuation. A limited effect of nonlocal material parameter was instead observed on the pull-in tip deflection. The comparative analysis of the theoretical outcomes obtained within the TPNL theory of elasticity, with available data of AS pointed out on a satisfactory accuracy of the models presented in the study, thus validating them and providing the most appropriate range of values of the local model fraction to be considered in the simulations according to the geometric parameters. The obtained results were thus particularly relevant for the accurate design of micro and nano-switches, according to the current trend of minimizing the size of devices as much as possible.

Author Contributions

G. Mikhasev initiated the project and suggested the model for a nano-switch based on the TPNL theory of elasticity; E. Radi proposed QDL model for distribution of the lateral force and conducted calculations for the freestanding beam; V. Misnik calculated a pull-in voltage accounting for intermolecular forces. The manuscript was written through the contribution of all authors. All authors discussed the results, reviewed, and approved the final version of the manuscript.

Acknowledgments

G.M. and V.M. would like to thank the Belarusian State University for support of the work carried out within the framework of the State Program of Scientific Research in the Republic of Belarus “Convergence-2025” (No. 1.7.01.2). E.R acknowledges Italian MIUR for support within the framework of the grant MIUR-PRIN 2020F3NCPX "Mathematics for industry 4.0 (Math4I4)".

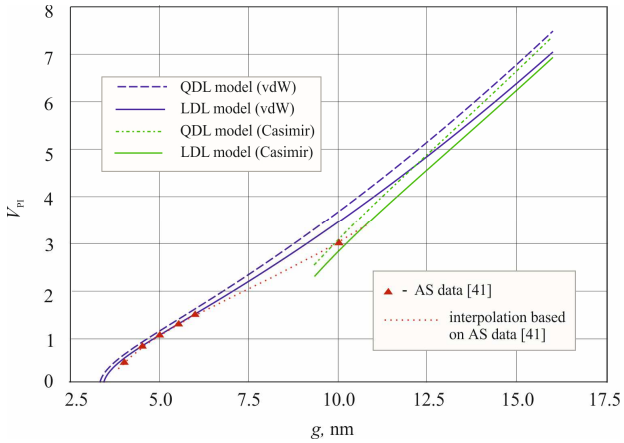


Fig. 12. Pull-in voltage V_{PI}, evaluated based on the LDL and QDL models and by using the atomistic simulation [41] taking the intermolecular forces into account, versus the gap g. Pull-in voltages found by the atomistic simulation [41] are marked in the plot.

Conflict of Interest

The authors declared no potential conflicts of interest concerning the research, authorship, and publication of this article.

Funding

Not Applicable.

Data Availability Statements

The datasets generated and/or analyzed during the current study are available from the corresponding author on reasonable request.

References

[1] Bruschi, P., Nannini, A., Paci, D., Pieri, F., A method for cross-sensitivity and pull-in voltage measurement of MEMS two-axis accelerometers, *Sensors and Actuators A: Physical*, 123-124, 2005, 185-193.
[2] Matmat, M., Koukos, K., Coccetti, F., Idda, T., Marty, A., Escriba, C. et al., Life expectancy characterization of capacitive RF MEMS switches, *Microelectronics Reliability*, 50(9-10), 2010, 1692-1696.
[3] De Volf, Van Spengen, W.M., Techniques to study the reliability of metal RF MEMS of capacitive switches, *Microelectronics Reliability*, 42(9-11), 2002, 1789-1794.
[4] Lin, W.H., Zhao, Y.P., Nonlinear behavior for nanoscale electrostatic actuators with Casimir force, *Chaos, Solitons and Fractals*, 23, 2005, 1777-1785.
[5] Cai1, T., Fang, Yu., Fang, Yi., Li, R., Yu, Y., Huang, M., Electrostatic pull-in application in flexible devices: A review, *Beilstein Journal of Nanotechnology*, 13, 2022, 390–403.
[6] Ke, C.H., Pugno, N., Peng, B., Espinosa, H.D., Experiments and modeling of carbon nanotube-based NEMS devices, *Journal of the Mechanics and Physics of Solids*, 53(6), 2005, 1314-1333.
[7] Loh, O.Y., Espinosa, H.D., Nanoelectromechanical contact switches, *Nature Nanotechnology*, 7(5), 2012, 283-295.
[8] Basu, S., Prabhakar, A., Bhattacharya, E., Estimation of stiction force from electrical and optical measurements on cantilever beams, *Journal of Microelectromechanical Systems*, 16(5), 2007, 1254-1262.
[9] Ramezani, A., Alasty, A., Akbari, J., Closed-form solutions of the pull-in instability in nanocantilevers under electrostatic and intermolecular surface forces, *International Journal of Solids and Structures*, 44, 2007, 4925-4941.
[10] Gusso, A., Delben, G.J., Dispersion force for materials relevant for micro-and nanodevices fabrication, *Journal of Physics D: Applied Physics*, 41 (17) (2008) 175405.
[11] Lamoreaux, S., The Casimir force: background, experiments, and applications, *Reports on Progress in Physics*, 68, 2005, 201236.
[12] Lin, W.H., Zhao, Y.P. Casimir effect on the pull-in parameters of nanometer switches, *Microsystem Technologies*, 11, 2005, 80-85.
[13] Soroush, R., Koochi, A., Kazemi, A.S., Noghrehabadi, A., Haddadpour, H., Abadyan, M., Investigating the effect of Casimir and van der Waals attractions on the electrostatic pull-in instability of nano-actuators, *Physica Scripta*, 82, 2010, 045801.
[14] Koochi, A., Kazemi, A.S., Beni, Y.T., Yekrangi, A., Abadyan, M., Theoretical study of the effect of Casimir attraction on the pull-in behavior of beam-type NEMS using modified Adomian method, *Physica E: Low-dimensional Systems and Nanostructures*, 43(2), 2010, 625–632.
[15] Radi, E., Bianchi, G., di Ruvo, L., Upper and lower bounds for the pull-in parameters of a micro- or nanocantilever on a flexible support, *International Journal of Non-Linear Mechanics*, 92, 2017, 176-186.
[16] Radi, E., Bianchi, G., di Ruvo, L., Analytical bounds for the electromechanical buckling of a compressed nanocantilever, *Applied Mathematical Modelling*, 59, 2018, 571-582.
[17] Bianchi, G., Radi, E., Analytical estimates of the pull-in voltage for carbon nanotubes considering tip-charge concentration and intermolecular forces, *Meccanica*, 55(1), 2020, 193-209.
[18] Radi, E., Bianchi, G., Nobili, A., Bounds to the pull-in voltage of a MEMS/NEMS beam with surface elasticity, *Applied Mathematical Modelling*, 91, 2021, 1211-1226.
[19] Goharimanesh, M., Koochi, A., Nonlinear oscillations of CNT nano-resonator based on nonlocal elasticity: The energy balance method, *Reports in Mechanical Engineering*, 2(1), 2021, 41-50.
[20] Malikan, M., Eremeyev, V.A., Sedighi, H.M., Buckling analysis of a non-concentric double-walled carbon nanotube, *Acta Mechanica*, 231, 2020, 5007-5020.
[21] Dastjerdi, S., Malikan, M., Mechanical analysis of eccentric defected bilayer graphene sheets considering the van der Waals force, *Proceedings of the Institution of Mechanical Engineers, Part N: Journal of Nanomaterials, Nanoengineering and Nanosystems*, 235(1-2), 2021, 44-51.
[22] Sedighi, H.M., Malikan, M., Valipour, A., ⊠ur, K.K., Nonlocal vibration of carbon/boron-nitride nano-hetero-structure in thermal and magnetic fields by means of nonlinear finite element method, *Journal of Computational Design and Engineering*, 7(5), 2020, 591-602.
[23] Jena, S.K., Chakraverty, S., Malikan, M., Sedighi, H., Implementation of Hermite–Ritz method and Navier's technique for vibration of functionally graded porous nanobeam embedded in Winkler–Pasternak elastic foundation using bi-Helmholtz nonlocal elasticity, *Journal of Mechanics of Materials and Structures*, 15(3), 2020, 405-434.
[24] Koochi, A., Goharimanesh, M., Gharib, M.R., Nonlocal electromagnetic instability of carbon nanotube-based nano-sensor, *Mathematical Methods in the Applied Sciences*, 2021, https://doi.org/10.1002/mma.7216.
[25] Abouelregal, A.E., Sedighi, H., Faghidian, S.A, Shirazi, A.H., Temperature-dependent physical characteristics of the rotating nonlocal nanobeams subject to a varying heat source and a dynamic load, *Facta Universitatis, Series: Mechanical Engineering*, 19(4), 2021, 633-656.
[26] Malikan, M., Eremeyev, V.A., On nonlinear bending study of a piezo-flexomagnetic nanobeam based on an analytical-numerical solution, *Nanomaterials*, 10(9), 2020, 1762.
[27] Malikan, M., Eremeyev, V.A., On a flexomagnetic behavior of composite structures, *International Journal of Engineering Science*, 175, 2022, 103671.
[28] Abdi, J., Koochi, A., Kazemi, A.S., Abadyan, M., Modeling the effects of size dependence and dispersion forces on the pull-in instability of electrostatic cantilever NEMS using modified couple stress theory, *Smart Materials and Structures*, 20, 2011, 055011.
[29] Rahaeifard, M., Kahrobaiyan, M., Asghari, M., Ahmadian, M., Static pull-in analysis of microcantilevers based on the modified couple stress theory, *Sensors and Actuators A: Physical*, 171, 2011, 370-374.
[30] Taati, E., Sina, N., Static Pull-in Analysis of Electrostatically Actuated Functionally Graded Micro- Beams Based on the Modified Strain Gradient Theory, *International Journal of Applied Mechanics*, 10(3), 2018, 1850031.
[31] Yang, J., Jia, X.L., Kitipornchai, S., Pull-in instability of nano-switches using nonlocal elasticity theory, *Journal of Physics D: Applied Physics*, 41, 2008, 035103-035111.
[32] Mousavi, T., Bornassi, S., Haddadpour, H., The effect of small scale on the pull-in instability of nano-switches using DQM, *International Journal of Solids and Structures*, 50(9), 2013, 11931202.
[33] Sedighi, H.M., Sheikhanzadeh, A., Static and dynamic pull-in instability of nano-beams resting on elastic foundation based on the nonlocal elasticity theory, *Chinese Journal of Mechanical Engineering*, 30, 2017, 385-397.
[34] Eringen, A.C., Theory of Nonlocal Elasticity and Some Applications, *Technical report, Princeton Univ NJ Dept of Civil Engineering*, 1984.
[35] Eringen, A.C., *Nonlocal Continuum Field Theories*, Springer Science & Business Media, 2002.
[36] Sadeghian, H., Yang, C.K., Goosen, J.F.L., van der Drift, E., Bossche, A., French, P.J., van Keulen, F., Characterizing size-dependent effective elastic modulus of silicon nanocantilevers using electrostatic pull-in instability, *Applied Physics Letters*, 94, 2009, 221903.
[37] Mikhasev, G.I., Free high-frequency vibrations of nonlocally elastic beam with varying cross-section area, *Continuum Mechanics and Thermodynamics*, 33, 2021, 1299-1312.
[38] Mikhasev, G., Nobili, A., On the solution of the purely nonlocal theory of beam elasticity as a limiting case of the two-phase theory, *International*

Journal of Solids and Structures, 190, 2020, 47-57.
[39] Mikhasev, G., Avdeichik, E., Prikazchikov, D., Free vibrations of nonlocally elastic rods, *Mathematics and Mechanics of Solids*, 24(5), 2019, 1279-1293.
[40] Romano, G., Barretta, R., Diaco, M., de Sciarra, F.M., Constitutive boundary conditions and paradoxes in nonlocal elastic nanobeams, *International Journal of Mechanical Sciences*, 121, 2017, 151-156.
[41] Dequesnes, M., Rotkin, S.V., Aluru, N.R., Calculation of pull-in voltages for carbon-nanotube-based nanoelectromechanical switches, *Nanotechnology*, 13, 2002, 120-131.
[42] Fernández-Sáez, J., Zaera, R., Vibrations of Bernoulli-Euler beams using the two-phase nonlocal elasticity theory, *International Journal of Engineering Sciences*, 119, 2017, 232-248.
[43] Mikhasev, G.I., A study of free high-frequency vibrations of an inhomogeneous nanorod, based on the nonlocal theory of elasticity, *Vestnik St. Petersburg University: Mathematics*, 54(2), 2021, 125-134.
[44] Akita, S., Nakayama, Y., Nanotweezers consisting of carbon nanotubes operating in an atomic force microscope, *Applied Physics Letters*, 79, 2001, 1691-1693.
[45] Wong, E.W., Sheehan, P.E., Lieber, C.M., Nanobeam mechanics elasticity, strength, and toughness of nanorods and nanotubes, *Science,* 277, 1997, 1971-1975.
[46] Van Lier, G., Van Alsenoy, C., Van Doren, V., Geerlings, P., Ab initio study of the elastic properties of single-walled carbon nanotubes and graphene, *Chemical Physics Letters*, 326(1-2), 2000, 181-185.
[47] Treacy, M.M.J., Ebbesen, T.W., Gibson, J.M., Exceptionally high Young's modulus observed for individual carbon nanotubes, *Nature*, 381, 1996, 678-680.
[48] Eringen, A.C., On differential equations of nonlocal elasticity and solutions of screw dislocation and surface waves, *Journal of Applied Physics*, 54, 1983, 4703-4710.
[49] Mikhasev, G., Botogova, M., Free localized vibrations of a long double-walled carbon nanotube introduced into an inhomogeneous elastic medium, Vestnik *St. Petersburg University: Mathematics,* 49(1), 2016, 85–91.

ORCID iD

Gennadi Mikhasev https://orcid.org/0000-0002-9409-9210
Enrico Radi https://orcid.org/0000-0002-7410-3008
Vyacheslav Misnik https://orcid.org/0000-0001-7519-3343

© 2022 Shahid Chamran University of Ahvaz, Ahvaz, Iran. This article is an open access article distributed under the terms and conditions of the Creative Commons Attribution-NonCommercial 4.0 International (CC BY-NC 4.0 license) (http://creativecommons.org/licenses/by-nc/4.0/).

How to cite this article: Mikhasev G., Radi E., Misnik V. Pull-in Instability Analysis of a Nanocantilever Based on the Two-Phase Nonlocal Theory of Elasticity, *J. Appl. Comput. Mech.*, xx(x), 2022, 1–11. https://doi.org/10.22055/jacm.2022.40638.3619

Publisher's Note Shahid Chamran University of Ahvaz remains neutral with regard to jurisdictional claims in published maps and institutional affiliations.